Depletion-mediated piezoelectric AlGaN/GaN resonators

Azadeh Ansari* and Mina Rais-Zadeh**

Department of Electrical Engineering and Computer Science, University of Michigan, 1301 Beal Avenue, Ann Arbor, MI 48109, USA

* Corresponding author: e-mail: azadans@umich.edu, Phone: +1 734 757 3188, Fax: +1 734 764-4249
** e-mail: minar@umich.edu, Phone: +1 734 764 4249

The electromechanical properties of an acoustic wave propagating in a piezoelectric media can be tuned by modulation of the resistivity of the piezoelectric material. This is readily available in piezoelectric semiconductor materials, wherein acoustic phonons and charge carriers can interact. In this work, we employ epitaxially grown AlGaN/ GaN heterostructures in bulk acoustic wave resonators with Schottky interdigitated transducers biased in the depletion region to study the interaction between piezoelectric strain and depletion charges. By modulating the impedance of the depletion layer upon application of DC voltages, we tune the acoustic properties of bulk-mode resonators and show significant Q enhancement as the result of a depletion force added to the piezoelectric actuation force. Furthermore, we compare the performance of such resonators with pure GaN piezoelectric resonators that have the same geometry but with the AlGaN layer removed. When integrated with AlGaN/GaN HEMTs (located on the acoustic cavity or next to the resonator), such resonators can be used as frequency references in oscillator circuits in radio frequency (RF) blocks or utilized in harsh environment sensing applications.

1 Introduction Epitaxially grown AlGaN/GaN heterostructures have attracted considerable attention recently due to their superior material properties. AlGaN/GaN high electron mobility transistors (HEMTs) are being widely used in power amplifiers in base stations and GaN-based LEDs comprise a large portion of the lighting market. As GaN exhibits strong piezoelectric properties, a number of groups have recently looked into GaN acoustic resonators and their integration with GaN electronic and optoelectronic components [1–6]. A very unique characteristic of GaN is the simultaneous presence of piezoelectricity with semiconducting properties, which allows for close investigation of interactions between acoustic phonons and charge carriers. In this work, we utilize high performance depletion-mediated bulk acoustic piezoelectric resonators, with Schottky interdigitated transducers (IDTs) deposited on top of an AlGaN/GaN layer. The actuation mechanism of such resonators consists of piezoelectric as well as electrostatic force caused by depletion forces. We show that significant Q enhancement of more than 240% is achieved with the application of electric field as a result of combined actuation mechanisms. Furthermore, by applying DC electric field to the Schottky transducers, efficient modulation of depletion capacitance and resistivity of the AlGaN layer is realized, causing 108 ppm of frequency tuning or increase in the acoustic velocity and more than 130% of improvement in transduction efficiency.

2 Fabrication and design Epitaxial AlGaN/GaN layers are grown on Si (111) substrate by metal-organic chemical vapor deposition (MOCVD). The total thickness of the GaN epi-layer is ∼1.8 μm and the AlGaN is 20 nm thick. Schottky contacts (Ni/Au) are deposited as IDT electrodes. Access to the two-dimensional electron gas (2DEG) at the AlGaN/GaN interface is provided by ohmic contacts (Ti/Al/Ti/Au) deposited outside of the active resonant region around the tethers and annealed at 800 °C in N_2 environment. Trenches are made to define the contours of the resonator by chlorine-based plasma etching of AlGaN/GaN. To form suspended membranes, the Si substrate is removed using xenon difluoride (XeF_2) isotropic etching from the front-side. More details about the epitaxial stack and fabrication process can be found in Ref. [7]. A scanning electron microscope (SEM) image and a cross-section schematic of the fabricated
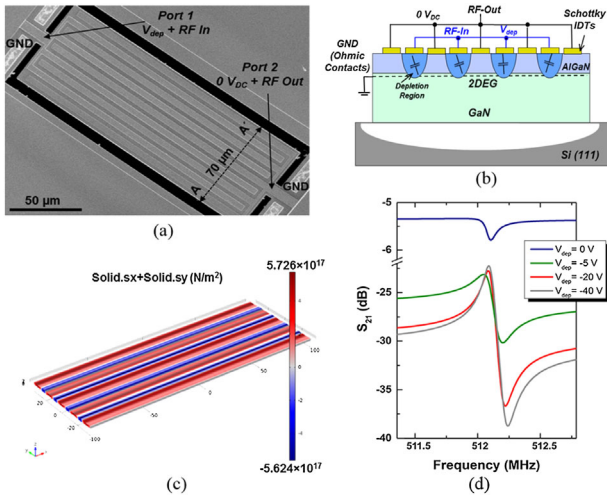
Figure 1 (a) An SEM image of the fabricated AlGaN/GaN resonator. (b) A cross-section schematic of the depletion-mediated resonator, where the input Schottky IDTs are biased in depletion and the output Schottky IDTs are biased at 0 V_{DC}. Access to 2DEG is provided via ohmic contacts biased at 0 V_{DC}. (c) COMSOL simulation of the stress profile of the ninth-order width-extensional resonance mode. (d) S_{21} frequency response at $P_{in} = -5$ dBm when the depletion voltage at the input port is varied from 0 to -40 V. The voltage at output port is kept at 0 V_{DC}. Mechanical Q increases from 3500 at -5 V to 5000 at -40 V.

AlGaN/GaN resonator is shown in Fig. 1(a and b). The resonator is 70 μm wide, consisting of nine IDT fingers, each 5 μm wide and spaced 3 μm apart. The device operates at its ninth-order width-extensional resonance mode at ~512 MHz. The mode shape and frequency response of the resonator are shown in Fig. 1(c and d).

3 Effect of DC voltage on acoustic properties The dependency of acoustic properties (resonance frequency, electromechanical coupling coefficient (k_t^2), mechanical Q, and $k_t^2 \times Q$) on DC voltage are shown in Fig. 2. To better understand such trends, we characterize the depletion region and study the effect of DC voltage on the depletion capacitance and resistivity of the AlGaN layer and its subsequent effect on the motional properties of AlGaN/GaN resonators. It is worth mentioning that the transduction mechanism in this work is different from previous work reported by the authors in Ref. [8], where 2DEG is used as the bottom electrode and thus the transduction is switched off when the 2DEG is pinched. Here, we rely on lateral electrical field excitation, thus the larger the depletion layer, the more efficient the transduction is. The dependency of Q and transduction efficiency on the depletion layer will be discussed in detail in the following sections.

Figure 2 shows that as the 2DEG channel gets more depleted, the resonance frequency increases, as well as the $k_t^2 \times Q$, which is a figure of merit for acoustic resonators. Figure 3 shows the modified diode-embedded Butterworth
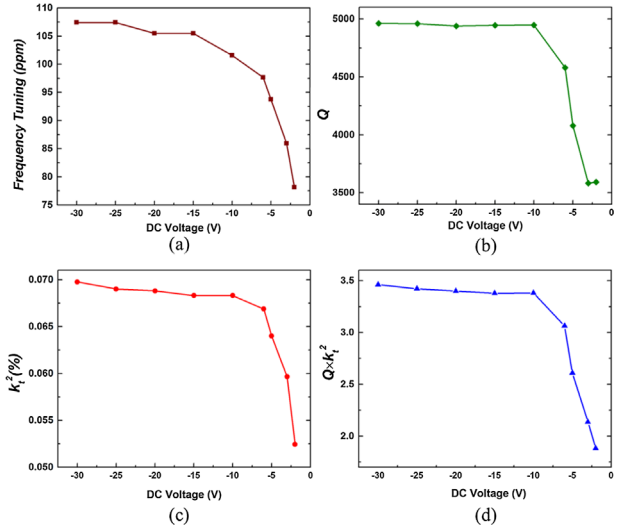

Figure 2 Dependency of acoustic properties of piezoelectric resonators on DC voltage at $P_{in} = -5$ dBm. (a) Frequency (or acoustic velocity) tuning, normalized to the resonance frequency at 0 V. (b) Mechanical Q, (c) electromechanical coupling coefficient (k_t^2), and (d) $k_t^2 \times Q$ versus DC voltage.

Van–Dyke (BVD) circuit model of the AlGaN/GaN resonator to explain the increase in *frequency* and $k_t^2 \times Q$ with DC voltage.

In this circuit model, the motional branch, as well as the electric components depend on applied electric field. R_m, L_m, and C_m for a width-extensional piezoelectric resonator with a width of W, length of L, and thickness of T can be estimated as [9]

$$R_m \approx \frac{\sqrt{M_{eq} \cdot k_{eff}}}{\eta^2 Q}, \tag{1}$$

$$L_m \approx \frac{M_{eq}}{\eta^2} = \left[\frac{\pi^4}{32} \frac{\rho}{} \frac{LT^3}{W} \frac{1}{d_{31}^2} \right] \frac{1}{k_{eff}^2}, \tag{2}$$

$$C_m \approx \frac{\eta^2}{k_{eff}} = \left[\frac{16}{\pi^4} \frac{W^2}{T^2} d_{31}^2 \right] k_{eff}, \tag{3}$$

where M_{eq} is the equivalent mass of the acoustic resonators ($M_{eq} = \rho \frac{WLT}{2}$), k_{eff} is the effective stiffness, η is the
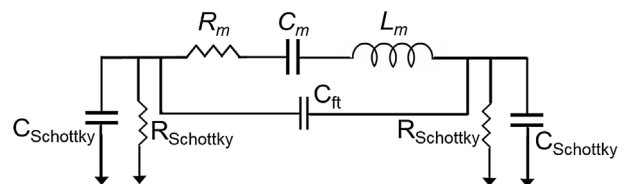

Figure 3 Diode-embedded equivalent circuit model of depletion-mediated AlGaN/GaN resonators.

Phys. Status Solidi A 213, No. 11 (2016)

Original

Paper

3009

electromechanical transduction efficiency, or in/output voltage to force transformation ratio. ρ is the density of the resonating material and d_{31} is the piezoelectric coefficient. R_m, L_m, and C_m depend on k_{eff}, which in turn depends on DC voltage, as discussed in Section 3.1. $C_{Schottky}$ and $R_{Schottky}$ denote the depletion capacitance and resistance of in/output Schottky IDTs which depend on the applied DC voltage. C–V and DC I–V characteristics of the Schottky contacts are shown in Fig. 4.

Two regimes are observed in the depletion region in the C–V profile shown in Fig. 4. In regime (i), the capacitance reflects the effective thickness of the Schottky barrier. As the 2DEG gets depleted and the charge is removed, the capacitance decreases. In regime (ii), the edge of the depletion layer has entered the high-resistivity GaN layer and the capacitance value has dropped significantly due to depletion of the 2DEG channel. Under zero external voltage biasing, the depletion layer extension in z-direction is determined by the thickness of the AlGaN layer, hence the junction capacitance is as follows:

$$C_0 = C_{j0} = n \times \frac{\varepsilon\varepsilon_0 A}{d}, \tag{4}$$

where n is the number of Schottky fingers ($n = 5$ for one IDT set), ε is the relative permittivity of the AlGaN layer, reported as (8–9.5) at low frequencies [10]. ε_0 is the free space permittivity, A is the area of each finger ($5 \times 200\,\mu m^2$), and d is thickness of the AlGaN layer (20 nm). Plugging in the measured value of 15 pF for C_0 at zero external voltage bias from Fig. 4 into Eq. (4), the relative permittivity of the AlGaN layer at 1 MHz is derived as 6.8, agreeing well with the reported values in Ref. [10]. The depletion width (Z_d) under Schottky contact for a uniformly doped sample is defined as [11, 12]

$$Z_d = \sqrt{\frac{2\varepsilon\varepsilon_0}{qN_d}(\Phi_b - V)}, \tag{5}$$

where q is electron charge, N_d is the carrier density, Φ_b is the barrier built-in potential, and V is the applied voltage. It must be noted that in a 2D heterostructure with quantum confinement, the carrier density is not uniformly distributed along the thickness (z-direction) of the AlGaN layer. Thus, Eq. (5) does not accurately model the extension of the depletion layer in regime (i) in z-direction. In order to gain additional information about the peak carrier concentration and its depth, particular to our AlGaN/GaN hetero-structure, we utilize the C–V profile shown in Fig. 4 to derive the carrier concentration (N_{CV}) as a function of depth (z_{CV}) in the depletion region based on the method discussed in Refs. [13, 14] and shown in Fig. 5(b).

$$N_{CV} = \frac{C^3}{q\varepsilon\varepsilon_0}\frac{dV}{dC}, \tag{6}$$

$$z_{CV} = \frac{\varepsilon\varepsilon_0}{C}, \tag{7}$$

where C is the measured capacitance in the C–V profile, when voltage (V) is applied to the Schottky contact. The 2DEG sheet carrier concentration can then be calculated as

$$n_s = \int_{-\infty}^{\infty} N_{CV}(z_{CV})dz_{CV}. \tag{8}$$

It is shown in Ref. [15] that the modulation of 2DEG density in AlGaN/GaN heterostructures causes significant increase in the generated strain as compared to the strain generated in GaN-only piezoelectric layers. Therefore, in order to achieve efficient transduction, it is beneficial to utilize IDTs on AlGaN/GaN heterostructures.

By applying a negative external bias, 2DEG charge starts to deplete. As the value of the negative voltage gets larger, the space charges get more depleted and at $V_{th} = -1.65$ V the depletion layer will completely penetrate through the 2DEG (pinch-off voltage). In regime (ii) where
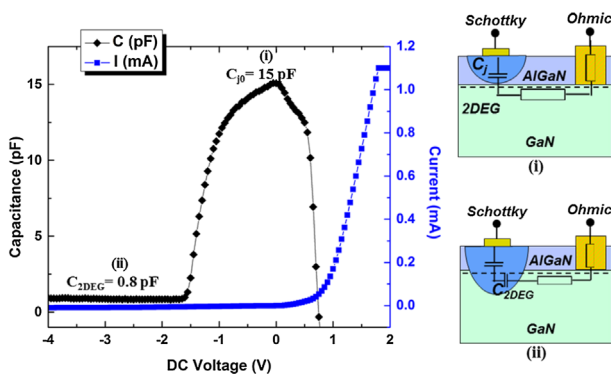

Figure 4 Schottky characteristics: C–V (measurement taken at 1 MHz) and DC I–V curves between one Schottky IDT set and ohmic GND. -1.65 V marks the threshold voltage at which point the depletion region pinches the 2DEG. 0.75 V marks the turn-on voltage of the Schottky diode. In case (i), at zero DC voltage, the depletion layer depth in the z-direction is set by the thickness of the AlGaN layer; in case (ii) the depletion layer has pinched the 2DEG sheet and penetrated into the high-resistivity GaN layer.
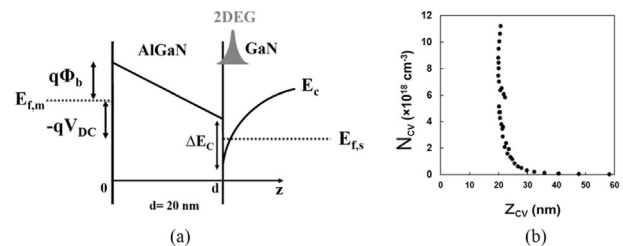

Figure 5 (a) Energy band diagram of the AlGaN/GaN hetero-structure under reverse bias condition. (b) Measured 2DEG carrier concentrations versus depth from the C–V profile in Fig. 4.

V_{dep} is smaller than $V_{pinch-off}$, the measured capacitance drops significantly, due to depletion of 2DEG charges. In regime (ii), extension of the depletion region in the GaN layer occurs under large depletion voltages and is known to cause reliability issues in AlGaN/GaN HEMTs [16]. It must be noted that the lateral extension of the depletion region as well as its further extension into the GaN layer, below the pinch-off voltage is not completely captured in the C–V measurement, explaining further improvement in the acoustic properties of laterally field excited resonators when $V_{dep} < V_{pinch-off}$.

3.1 Acoustic velocity It has been shown that the velocity of acoustic wave propagation in a piezoelectric semiconductor is dependent on the resistivity of the medium [17]. In Ref. [17], White et al. took advantage of such a phenomenon in surface acoustic waves (SAWs) to build delay lines with variable velocity of transmission by modulating the resistivity of the piezoelectric semiconductor material.

In the width-extensional AlGaN/GaN bulk-acoustic resonator, shown in Fig. 1(a), the acoustic velocity increases at larger depletion voltages. Figure 2(a) shows this trend. The increase in the acoustic velocity is attributed to an increase in the effective stiffness of the resonant structure as the AlGaN layer gets depleted of the carrier charges and thus becomes more resistive. Qualitatively, a piezoelectric material with higher resistivity can tolerate a larger electric field, whereas in a conductive piezoelectric material, the effect of the electric field is screened. As piezoelectric strain depends on the voltage applied to the piezoelectric material, a material with higher resistivity is effectively stiffer than its conductive counterpart under an applied electric field. Hence, larger resonance frequencies and acoustic velocities are expected with larger depletion voltages:

$$\omega = \sqrt{\frac{k_{eff}}{M_{eq}}}, \quad \upsilon = \sqrt{\frac{k_{eff}}{\rho}}, \tag{9}$$

$$k_{eff} = k\left(1 + \frac{K^2}{1 + \left(\frac{\sigma}{\omega\varepsilon\varepsilon_0}\right)^2}\right), \tag{10}$$

where ω is the fundamental angular resonance frequency, υ is the acoustic velocity, k is the stiffness under super conductivity conditions, K^2 is the electromechanical coupling coefficient of the piezoelectric material, σ is the conductivity of the material [17].

As shown in Fig. 2, the increase in the acoustic velocity is ~108 ppm, translating into ~0.021% of change in the effective stiffness. This rather small tuning is due to the fact that the modulation of the resistivity (and thus stiffness) occurs in the depletion region merely, which comprises only ~6% of the entire GaN-based resonant stack in the thickness direction. In order to significantly modulate the acoustic velocity in bulk-mode resonators, the thickness of the resonator should be thinned down to dimensions in the same order of the depletion layer depth.

Finally, to verify that the added stiffness is indeed due to charge modulation in the depletion layer and distinguish it from the standard piezoelectric frequency tuning with DC bias, we characterize a GaN bulk acoustic resonator in Section 4. The standard piezoelectric frequency tuning originates from the dependency of R_m, L_m, and C_m on the resonator dimensions (Eqs. (1)–(3)), which changes under DC bias as well as the dependency of d_{31} piezoelectric coefficient on DC bias [9]. It is seen that the effect of purely piezoelectric frequency tuning is negligible compared to the effect of k_{eff} tuning in depletion-mediated AlGaN/GaN resonators.

3.2 Electromechanical coupling For efficient electromechanical actuation, it is important to keep the Schottky actuators in the depletion region or in the reverse bias region in the case of p–n junctions. As piezoelectric strain is proportional to the electric field across the junction, lowering the resistance via forward or excessive reverse biasing of the diode screens the electric field and leads to a reduction of actuation efficiency. The dependency of k_t^2 on DC voltage is studied in Fig. 2(b). As expected, more efficient transduction is achieved when the actuation layer is more resistive.

Effective electromechanical coupling coefficient, defined as the ratio of the stored mechanical energy to the total input energy [18], is estimated as

$$k_t^2 \approx \frac{C_m}{C_0}, \tag{11}$$

where C_m is the motional capacitance and C_0 is the total static equivalent capacitance between the input and output ports, setting the feed-through level is S_{21} transmission response. C_m is proportional to stiffness as indicated by Eq. (3). In depletion-mediated resonators, both C_m and C_0 change with DC voltage. In fact, the effect of change in C_0 on k_t^2 is more pronounced in the two distinct regimes in the depletion region compared to the effect of C_m change. The transduction efficiency is maximized when the channel is fully pinched and C_0 is minimum.

Using $C_m = 0.25$ aF from MBVD fitting, and $C_0 = 0.35$ pF from direct C–V measurement between the input and output Schottky IDTs, k_t^2 is extracted as 0.07% at $V_{dep} = -30$ V, which agrees well with the measured k_t^2 shown in Fig. 2(c).

3.3 Q enhancement It has been shown in Ref. [19] that Q in bulk-mode GaN resonators depends on DC electric field, via phonon–electron interactions in such materials. Similarly, in AlGaN/GaN resonators, upon application of negative DC voltage to the Schottky contacts, the charge carriers are removed from the surface of the AlGaN layer and thus the loss associated with phonon–electron scattering in piezoelectric semiconductor materials is reduced. Furthermore, an increase in Q is reported when negative DC voltage is

Phys. Status Solidi A 213, No. 11 (2016)

Original

Paper

3011

applied to Schottky contacts in AlGaN/GaN heterostructures in Ref. [20], where the Q enhancement is attributed to increased stress in the thin films through an increased piezoelectric actuation of the Schottky barrier. In other words, Q increases due to the added stiffness in such resonators. While all the aforementioned phenomena may contribute to Q-enhancement in AlGaN/GaN resonators, in this work, the significant Q and insertion loss enhancement at large negative DC voltages, are attributed to combination of depletion and piezoelectric actuation forces. The dependency of Q on input power further proves that such mechanism is indeed dominant in AlGaN/GaN resonators in this work.

Figure 6 shows the frequency response of the depletion-mediated resonator when driven at input power level of $P_{in} = +10\,dBm$. While the feed-through level is the same for different DC voltages (unlike Fig. 1(d)), improvement in the insertion loss only occurs at the frequency of resonance. To explain the Q enhancement at high input power levels, we investigate the actuation mechanism of depletion-mediated piezoelectric resonators. Two mechanisms contribute to the actuation of such resonators, (i) the force caused by piezoelectric strain proportional to the z-component of the lateral electric field (E_z): $e_{31} = E_z \cdot d_{31}$ and (ii) modulation of depletion impedance of the depleted AlGaN/GaN layer [21]. The second contributor is negligible at low RF input power levels or low frequencies, however, as the input power increases, the depletion layer changes significantly with the same frequency as the frequency of actuation. Therefore, an electrostatic force is generated and added to the initial piezoelectric force. PN diode resonators based on depletion forces operate based on such mechanism [22, 23]. Depletion-mediated piezoelectric semiconductors have the advantage of combining both actuation mechanisms, thus
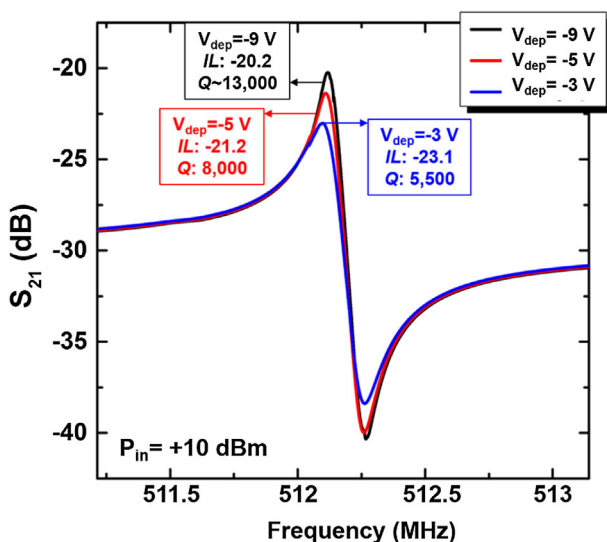
improving the Q factor significantly. The added electrostatic force is due to charge modulation upon application of AC voltage to the Schottky IDTs.

Figure 7 shows the carrier concentration versus depth from AlGaN surface, when AC voltage is applied in addition to the negative DC voltage. The depletion width in z-direction is set by AlGaN thickness ($\sim 20\,nm$) at zero DC voltage. The 2DEG carrier density is modulated with AC voltage. The charge modulation gives rise to modulation of electric field and thus electrostatic actuation force. As the charge distribution is not uniform in the z-direction, the generated electrostatic force component is derived in Eq. (12).

$$dF(z) = q_v AE dz = qN_{CV}(z)A \frac{\int_{z_d}^{z} qN_{CV}(z)dz}{\varepsilon \varepsilon_0} dz, \quad (12)$$

where q_v is the charge per unit volume, $N_{CV}(z)$ is the carrier concentration derived from Eq. (6), and A is the area of the depletion layer. z_d and z denote the depth of the depletion layer at V_{DC} and $V_{DC} + v_{AC}$, respectively (Fig. 7).

In the case of uniform carrier density distribution, we can model the depletion layer actuation force as shown in Eq. (13). Such equation is used in p–n junction and Schottky actuators reported in Refs. [22, 23]. In the case of AlGaN/GaN resonators, once the depletion layer has fully pinched the 2DEG and penetrated into the GaN layer, Eq. (13) can be used to model the depletion force, given that the depletion layers reside in the GaN layer (Fig. 8).

$$dF(z) = q_v AE dz = \frac{Aq^2 N_d^2}{\varepsilon \varepsilon_0}(z - z_d)dz, \quad (13)$$

where E is the electric field and Z_d is the depletion width when no AC signal is applied, N_d is the background carrier concentration in the GaN layer and A is the area of the

Figure 6 Q amplification and IL enhancement at frequency of resonance for $P_{in} = +10\,dBm$. Modulation of the impedance of the depletion layer with a frequency equal to the actuation frequency creates an electrostatic force, which adds to the piezoelectric force only at the frequency of resonance.
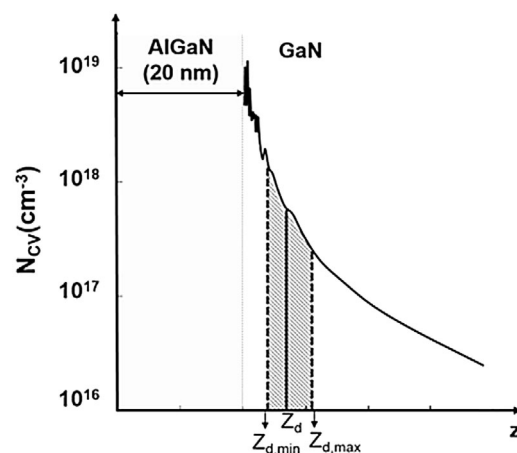

Figure 7 Carrier concentration versus depth from the AlGaN surface in AlGaN/GaN heterostructure. The dashed lines show charge modulation when AC signal is applied in addition to a negative DC voltage to the Schottky contact.
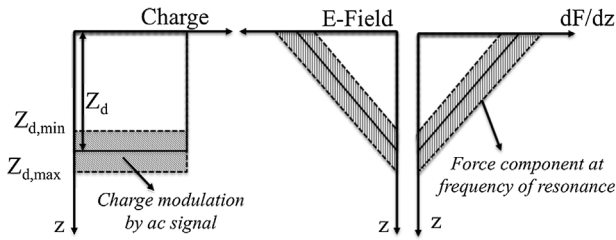
Figure 8 Charge, electric field, and force component of depletion-mediated resonators with uniformly distributed charge carriers. $Z_{d,min}$ and $Z_{d,max}$ denote the minimum and maximum depletion widths when AC signal is applied [23, 24].

depletion layer. Also, such model holds true in AlGaN/GaN resonators for estimation of lateral extension of depletion layer as the charge carrier distribution is assumed uniform in the lateral direction but a function of the depth from the AlGaN surface as shown in Fig. 7.

4 Standard GaN piezoelectric resonators with lateral field excitation This class of acoustic resonators are used as control experiments to compare the effect of Schottky contacts in depletion-mediated AlGaN/GaN resonators with standard lateral electric field piezoelectric GaN resonators. These devices have the same geometry as the AlGaN/GaN resonators discussed previously except that 20 nm-thick AlGaN layer is removed by a chlorine-based plasma etch. GaN layer is used as the active piezoelectric layer where two sets of IDT electrodes are deposited on top of it. As there is neither a bottom metal electrode, nor the 2DEG sheet, ohmic contacts for accessing the ground bottom electrode are not required in this case. The ninth-order width extensional resonance mode is shown in Fig. 9(a) and is at a slightly higher resonance frequency of 520 MHz due to reduction of the resonator mass by removal of the AlGaN layer as shown in Eq. (1).

DC voltage affects the stiffness and permittivity of any piezoelectric material (not only piezoelectric semiconductors) and hence their resonance frequency. To separate this effect from the frequency tuning in depletion-mediated resonators shown in Fig. 2(a), we study the effect of DC voltage on a standard GaN resonator in Fig. 9. The frequency tuning shows a linear trend and is only ~17 ppm at −40 V. This shows that depletion-mediated resonators are able to modulate the stiffness of the resonant stack more efficiently than their purely piezoelectric counterparts. Due to the combined depletion and piezoelectric actuation force, Q and insertion loss of the depletion-mediated piezoelectric resonators are more sensitive to DC voltage as compared to the pure GaN resonators. The dependency of Q of standard GaN resonators on DC voltage is attributed to reduction of charge trapping effects as well as removal of charge carriers upon application of DC voltage. This reduces the loss associated with phonon–electron scattering in piezoelectric semiconductors.
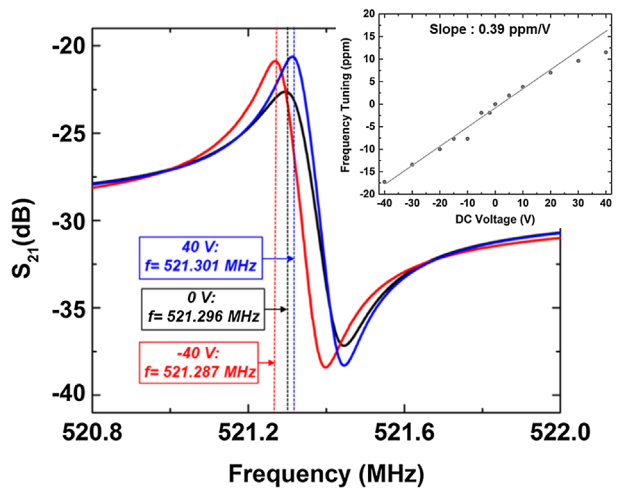
(a)
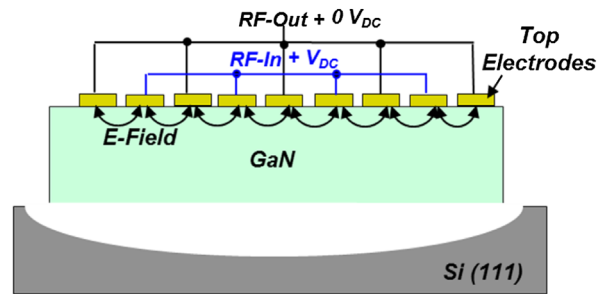
(b)

Figure 9 (a) S_{21} frequency response of the ninth-order width-extensional resonance mode of GaN resonator when 2DEG is removed. The voltage applied between two adjacent electrodes are −40, 0, and +40 V. Inset shows small fractional resonance frequency change with applied DC voltage. The slope of the frequency tuning versus DC voltage is 0.39 ppm V^{-1}, corresponding to piezoelectric tuning effect. (b) Cross section schematic of the lateral-field-excited GaN resonator.

5 Conclusions In this work, we investigated the performance of high-Q depletion-mediated AlGaN/GaN bulk acoustic resonators at different DC bias voltages. We show that for efficient actuation, the AlGaN layer needs to be biased in depletion, wherein depletion forces generated due to the modulation of the impedance of the depletion layer add up to the piezoelectric actuation force, causing a significant enhancement in Q and improvement of insertion loss. Furthermore, we characterized the dependency of the acoustic properties of bulk-mode resonators on the depletion layer. Finally, GaN-only piezoelectric resonators were compared with AlGaN/GaN depletion-mediated resonators to compare the effect of transduction via Schottky contacts on AlGaN/GaN heterostructures with acoustic performance of piezoelectric GaN resonators.

Original

Paper

Phys. Status Solidi A 213, No. 11 (2016)   3013

References

[1] M. Rais-Zadeh, V. Gokhale, A. Ansari, M. Faucher, D. Theron, Y. Cordier, and L. Buchaillot, GaN as an electromechanical material, IEEE J. Microelectromech. Syst. (JMEMS) **23**(6), 1252–1271 (2014).

[2] A. Ansari and M. Rais-Zadeh, Frequency Tunable Current-assisted AlGaN/GaN acoustic resonators, IEEE International Conference on Microelectromechanical Systems (MEMS 2016), Shanghai, China, January 2016.

[3] M. Faucher, Y. Cordier, M. Werquin, L. Buchaillot, C. Gaquiere, and D. Theron, Electromechanical transconductance properties of a GaN MEMS resonator with fully integrated HEMT transducers, J. Micromech. Syst. (JMEMS) **21**(2), 370–378 (2012).

[4] L. C. Popa and D. Weinstein, L-band Lamb mode resonators in gallium nitride MMIC technology, IEEE Frequency Control Symposium (FCS 2014), Taipei, Taiwan, May 2014.

[5] F. Niebelschuetz, K. Brueckner, K. Tonisch, R. Stephan, V. Cimalla, O. Ambacher, and M. Hein, Piezoelectrically-actuated epitaxially-grown AlGaN/GaN resonators, Phys. Status Solidi C **7**(7–8), 1829–1831 (2010).

[6] S. Vittoz, L. Rufer, G. Rehder, U. Heinle, and P. Benkart, Analytical and numerical modelling of AlGaN/GaN/AlN heterostructure based cantilevers for mechanical sensing in harsh environments, Sens. Actuators A **172**, 27–34 (2011).

[7] A. Ansari, R. Tabrizian, and M. Rais-Zadeh, A high-Q AlGaN/GaN phonon trap with integrated HEMT read-out, International Conference on Solid-State Sensors, Actuators and Microsystems (Transducers'15), Anchorage, Alaska, June 2015, pp. 2256–2259.

[8] A. Ansari and M. Rais-Zadeh, A thickness-mode AlGaN/GaN resonant bod high electron mobility transistor, IEEE Trans. Electron Devices **61**(4), 1006–1013 (2014).

[9] G. Piazza, P. J. Stephanou, and A. P. Pisano, Piezoelectric aluminum nitride vibrating contour-mode MEMS resonators, J. Microelectromech. Syst. (JMEMS) **15**(6), 1406–1418 (2006).

[10] C. Hong, L. Wu, T. Corrigan, W. Zhan-Guo, Z. Jian-Zhi, L. Zhao-Jun, Z. Yu, and L. Yuan-Jie, Determination of the relative permittivity of the strained AlGaN barrier layer in AlGaN/GaN heterostructures, Chin. Phys. B **18**(9), 3980–3984 (2009).

[11] P. Javorka, Fabrication and characterization of AlGaN/GaN high electron mobility transistors, PhD Thesis, RWTH, Aachen, Germany (2004).

[12] Z. Miao and L. Xin-Yu, Analysis of capacitance-voltage-temperature characteristics of GaN high-electron-mobility transistors, Chin. Phys. Lett. **32**(4), 048501 (2015).

[13] O. Ambacher, B. Foutz, J. Smart, J. Shealy, N. Weimann, K. Chu, M. Murphy, A. Sierakowski, W. J. Schaff, L. Eastman, R. Dimitrov, A. Mitchell, and M. Stutzmann, Two-dimensional electron gases induced by spontaneous and piezoelectric polarization in undoped and doped AlGaN/GaN heterostructures, J. Appl. Phys. **87**(1), 334–344 (2000).

[14] O. Ambacher, J. Smart, J. Shealy, N. Weimann, K. Chu, M. Murphy, W. Schaff, and L. Eastman, Two-dimensional electron gases induced by spontaneous and piezoelectric polarization charges in N- and Ga-face AlGaN/GaN heterostructures, J. Appl. Phys. **85**(6), 3222–3233 (1999).

[15] L. Shao, Active acoustic emission from a two-dimensional electron gas, PhD Thesis Dissertation, University of Michigan, Ann Arbor 2014.

[16] R. Vetury, N. Zhang, S. Keller, and U. Mishra, The impact of surface states on the DC and RF characteristics of AlGaN/GaN HFETs, IEEE Trans. Electron Devices **48**(3), 560–566 (2001).

[17] D. L. White, Ultrasonic wave transmission device utilizing semiconductor piezoelectric material to provide selectable velocity of transmission, US Patent 3200354 (August 1959).

[18] V. Kaajakari, Theory M.E.M.S. analysis of resonators IEEE Ultrasonics, Ferroelectrics and Frequency Control (UFFC) Tutorials, 2005.

[19] V. J. Gokhale and M. Rais-Zadeh, Phonon-electron interactions in piezoelectric semiconductor bulk acoustic wave resonators, Sci. Rep. **4**, 5617 (2014). DOI: 10.1038/srep05617.

[20] K. Tonisch, C. Buchheim, F. Niebelschütz, A. Schober, G. Gobsch, V. Cimalla, O. Ambacher, and R. Goldhahn, Piezoelectric actuation of GaN/AlGaN/(GaN) heterostructures, J. Appl. Phys. **104**, 084516 (2008).

[21] S. Masmanidis, R. Karabalin, I. De Vlaminck, G. Borghs, M. Freeman, and M. Roukes, Multifunctional nanomechanical systems via tunably coupled piezoelectric actuation, Science **317**(5839), 780–783 (2007).

[22] J. Ransley, C. Durkan, and A. Seshia, Silicon depletion layer actuators, Appl. Phys. Lett. **92**, 184103 (2008).

[23] E. Hwang and S. A. Bhave, Transduction of high-frequency micromechanical resonators using depletion forces in p-n diodes, IEEE Trans. Ultrason. Ferroelectr. Freq. Control **57**(7), 1664–1672 (2010).

[24] S. M. Sze, Semiconductor Devices: Physics and Technology (Wiley, New York, 2002).